SPANDIDOS PUBLICATIONS

INTERNATIONAL JOURNAL OF ONCOLOGY 63: 96, 2023

Overexpression of SERPINA3 suppresses tumor progression by modulating SPOP/NF-κB in lung cancer

YANXIA JIN[1], YUEYANG ZHANG[1], ANKANG HUANG[2], YING CHEN[1], JINSONG WANG[1], NA LIU[1], XIANPING WANG[1], YONGSHENG GONG[2], WEIDONG WANG[1] and JICHENG PAN[1]

[1]Hubei Key Laboratory of Edible Wild Plants Conservation and Utilization, College of Life Sciences, Hubei Normal University, Huangshi, Hubei 435002; [2]Suzhou Municipal Hospital, The Affiliated Suzhou Hospital of Nanjing Medical University, Suzhou, Jiangsu 215002, P.R. China

Received February 2, 2023; Accepted June 23, 2023

DOI: 10.3892/ijo.2023.5544

Abstract. The pathogenesis mechanism of lung cancer is very complex, with high incidence and mortality. Serpin family A member 3 (SERPINA3) expression levels were reduced in the sera of patients with lung cancer and may be a candidate diagnostic and prognostic survival biomarker in lung cancer, as previously reported. However, the detailed biological functions of SERPINA3 in the pathogenesis of lung cancer remain unknown. In the present study, it was aimed to explore the effects of SERPINA3 on the occurrence of lung cancer. SERPINA3 expression was assessed using bioinformatics database analysis and experimental detection. Then, the biological effects of SERPINA3 were investigated in a cell culture system and a xenograft model of human lung cancer. The potential regulatory mechanism of SERPINA3 in lung cancer was explored by data-independent acquisition mass spectrometry (DIA-MS) detection and further validated by western blotting (WB). The results indicated that SERPINA3 expression levels were significantly downregulated in lung cancer tissues and cell lines. At the cellular level, it was revealed that overexpressed SERPINA3 inhibited cell growth, proliferation, migration and invasion and promoted the apoptosis of lung cancer cells. Moreover, overexpressed SERPINA3 enhanced the sensitivity of lung cancer cells to osimertinib. *In vivo*, a xenograft model of human lung cancer was established with BALB/c nude mice. After the injection of A549 cells, the tumor growth of the tumor-bearing mice in the SERPINA3-overexpressing group increased more slowly, and the tumor volume was smaller than that in the empty-vector group. Mechanistically, a total of 65 differentially expressed proteins were identified. It was found that the speckle-type POZ protein (SPOP) was significantly upregulated in SERPINA3-overexpressing H157 cells using DIA-MS detection and analysis. WB validation showed that SPOP expression increased, and NF-kappaB (NF-κB) p65 was inhibited in cell lines and tumor tissues of mice when SERPINA3 was overexpressed. The present findings suggest that SERPINA3 is involved in the development of lung cancer and has an antineoplastic role in lung cancer.

Correspondence to: Professor Jicheng Pan or Professor Weidong Wang, Hubei Key Laboratory of Edible Wild Plants Conservation and Utilization, College of Life Sciences, Hubei Normal University, 11 Cihu Road, Huangshi, Hubei 435002, P.R. China
E-mail: panproteins@email.hbnu.edu.cn
E-mail: wangweidong@hbnu.edu.cn

Abbreviations: SERPINA3, serpin family A member 3, Alpha-1-antichymotrypsin; DIA-MS, data-independent acquisition mass spectrometry; SPOP, speckle-type POZ protein; NSCLC, non-small cell lung cancer; LUAD, lung adenocarcinoma; LUSC, lung squamous cell carcinoma; DEPs, differentially expressed proteins; CCK-8, Cell Counting Kit-8; EdU, 5-ethynyl-2'-deoxyuridine; RT-qPCR, reverse transcription-quantitative PCR

Key words: SERPINA3, lung cancer, cell proliferation, animal model, DIA-MS, SPOP, NF-kappaB

Introduction

Lung cancer is a primary malignant tumor originating from the bronchial mucosal epithelium, with 11.4% of morbidity and 18% of mortality in the world according to global cancer statistics in 2020 (1), of which ~76% are non-small cell lung cancer (NSCLC) and 13% are small cell lung cancer according to clinicopathological characteristics (2). NSCLC mainly includes lung adenocarcinoma (LUAD) and lung squamous cell carcinoma (LUSC) based on histologic subtypes. LUAD is derived from pulmonary peripheral tissue lesions, accounts for 40% of patients with lung cancer (3) and is asymptomatic in the early stage. LUSC is derived from proximal airway epithelial cells, which are sensitive to chemoradiotherapy (4). LUAD and LUSC are both genetically altered and associated with poor prognosis (5). The pathogenesis of lung cancer remains poorly understood, and genetic factors and immune and signaling pathways are involved in its occurrence and development (6,7). Targeting these genes or signaling pathways and regulating the immune system, numerous inhibitors or targeted drugs have been developed to improve the treatment of lung cancer in clinics (8,9). However, due to the tumor immune microenvironment and its heterogeneity (10), susceptibility to drug resistance, local invasion and distant metastasis (11), the five-year survival rate of lung cancer is <15% (12,13). Therefore, it is crucial to elucidate the pathogenesis

of lung cancer, which will be helpful for drug development to improve the survival of patients with lung cancer.

The SERPINA3 gene, with 1,272 base sequences in *Homo sapiens*, encodes a protein named alpha-1-antichymotrypsin with a molecular weight of ~47 kDa. SERPINA3 is a serpin peptidase inhibitor and a member of the acute phase protein family that is synthesized in the liver and secreted into the blood (14) and plays essential roles in pathological processes (15), including the inflammatory response (16,17), immunotherapy response (18), cardiovascular disease (19), and in neurodegenerative diseases such as Alzheimer's syndrome (20). Notably, studies have reported that SERPINA3 expression levels or glycosylation levels are abnormal in tumors and could be a biomarker for the diagnosis of tumors such as liver cancer (16,21). Moreover, it was found that the expression level of SERPINA3 was also associated with the survival of patients with cancer and may be a therapeutic target for tumor treatment (16). For example, Lara-Velazquez *et al* (22) reported that knockdown of SERPINA3 inhibited tumor growth in glioma *in vitro* and *in vivo*, suggesting that SERPINA3 could be a target for the treatment of glioma. Zhu *et al* (23) found that SERPINA3 acted as a tumor suppressor in liver cancer and inhibited the development and metastasis of liver cancer, suggesting that SERPINA3 could be used as a target for treatment intervention in liver cancer. Zhang *et al* (24) reported that overexpression of SERPINA3 promotes tumor invasion and migration in triple-negative breast cancer cells.

As previously reported by the authors, it was found that glycosylated SERPINA3 could be used as a candidate diagnostic biomarker in early NSCLC and that it could also significantly improve the specificity of carcinoembryonic antigen (25,26). It was also discussed that SERPINA3 may be a biomarker for the prognostic survival of patients with lung cancer (16). It was also found that SERPINA3 could be used to distinguish malignant from benign lung lesions with an AUC value of 0.806 (Fig. S1). To use SERPINA3 as a promising biomarker, it is necessary to improve understanding of its effects on pathogenesis and the molecular basis of lung cancer (27,28). However, the detailed biological functions of SERPINA3 involvement in the occurrence of lung cancer remain unknown.

In the present study, it was aimed to investigate the biological roles of SERPINA3 in the pathogenesis of lung cancer. Firstly, the expression of SERPINA3 in lung cancer was measured with tissue samples and cell samples and then the effects of SERPINA3 on the pathogenesis of lung cancer were explored through the construction of stable SERPINA3-overexpressing lung cancer cells at the cellular and animal levels. Moreover, data-independent acquisition mass spectrometry (DIA-MS) for quantitative proteomics detection was designed to explore the regulatory mechanism of SERPINA3 involved in the development of lung cancer. Furthermore, the differentially expressed proteins (DEPs) regulated by overexpressed SERPINA3 in lung cancer cells were analyzed and screened with bioinformatics analysis. Finally, the DEPs were validated by western blotting (WB) in cell experiments and *in vivo* models to investigate the possible regulatory mechanism.

Materials and methods

Clinical samples collection. The patient was enrolled based on CT imaging data and tumor biomarker screening results at the Suzhou Municipal Hospital of Nanjing Medical University. The present study was approved (approval no. KL901372) by the Ethics Committee of Suzhou Municipal Hospital (Suzhou, China). Written informed consents were obtained from all participants. All patients were diagnosed upon histopathological analyses. The patients with lung cancer were graded using the eighth edition of the TNM classification of the International Association for the Study of Lung Cancer (IASLC). Preoperative serum samples of 243 cases were selected and collected to detect SERPINA3 expressions in serological level, of which 64 patients with benign diseases and 179 patients with lung cancer. The fresh tissue samples were collected from patients with lung cancer between June 2021 and June 2022, which were used to validate the protein expression level of SERPINA3. The information on serum and tissue samples is also listed in Table SI. The collected tissues were frozen with liquid nitrogen, of which the tumor sizes were <3 cm, and the paracancerous tissues were 2 cm away from the tumor tissues. The tissue samples were lysed with radioimmunoprecipitation assay (RIPA) lysis buffer (cat. no. P00138; Beyotime Institute of Biotechnology) containing 50 mM Tris (pH 7.4), 150 mM NaCl, 1% Triton X-100, 1% sodium deoxycholate, 0.1% SDS and 1 mM phenylmethylsulfonyl fluoride, and ceramic beads were added for automatic crushing. The supernatant, namely, tissue samples' protein extract, was harvested after centrifugation at 4˚C, 15,294 x g for 10 min with centrifugal machine (Eppendorf 5804R).

Cells and cell culture. The human lung cancer cell lines A549 (cat. no. CL-0016), H157 (cat. no. CL-0388) and NCI-H1437 (cat. no. CL-0631) were kindly provided by the Procell Life Science & Technology Co., Ltd., and the NCI-H1975 cells (cat. no. BNCC340345) were purchased from the BeNa Culture Collection. These cell lines were detected by STR authentication. The cells were sustained in DMEM or RPMI-1640 medium containing 10% fetal bovine serum (GIBCO, Invitrogen; Thermo Fisher Scientific, Inc.) and 1% penicillin-streptomycin sulfate (Invitrogen; Thermo Fisher Scientific, Inc.). All cells were cultivated at 37˚C in a 5% CO_2 atmosphere.

Construction of the stable cell lines of overexpressed SERPINA3 in lung cancer cells. To investigate the biological effects of SERPINA3 on lung cancer, the stable cell lines of overexpressed SERPINA3 in lung cancer cells were constructed, and the recombinant overexpression vector and stable cells were prepared as previously described (29,30). Briefly, the human SERPINA3 plasmid (gene ID: 12; NCBI accession: NM_001085) was ligated into the pCDH-CM V-MCS-EF1-copGFP-T2A-Puro control vector with the restriction endonuclease *Xba*I site (TCTAGA) and *Not*I site (GCGGCCGC). The lentivirus package was produced by recombinant overexpression plasmid incubated with psPAX2 vector and pMD2.G vector. The lentivirus vector carrying the empty-vector was used as a negative control. The DNA was incubated with lipofectamine 2000 (Invitrogen; Thermo Fisher Scientific, Inc.) for 20 min at room temperature and transfected into the 293T cells (BeNa Culture Collection). Subsequently, the lentivirus was harvested. The harvested lentivirus particles were used to infect the three kinds of

lung cancer cell lines for 48 h, and the stably overexpressed SERPINA3 lung cancer cells were selected by culturing in a medium containing 2 μg/ml puromycin.

Reverse transcription-quantitative PCR (RT-qPCR). The RT-qPCR experiments were used to detect whether SERPINA3 was overexpressed in stable-transfected lung cancer cell lines. Total RNA was extracted from the lung cancer cells after overexpression of SERPINA3 with the TRIzol reagent (cat no. 15596026; Invitrogen; Thermo Fisher Scientific, Inc.) Then, cDNA was synthesized from total RNA with 500 ng oligo (dT), 10 mM dNTPs and the M-MLV reverse transcriptase (cat no. AE101-03; TransGen Biotech Co., Ltd.) in 5X first chain synthetic buffer. Thermocycling conditions for reverse transcription were as follows: 50 min at 37˚C for cDNA synthesis and 15 min at 70˚C for stopping the reaction. All qPCR reactions contained 100 ng cDNA and thermocycling conditions were as follows: 30 sec at 95˚C for initial denaturation, followed by forty cycles of 10 sec at 95˚C and 30 sec at 60˚C and 30 sec at 72˚C. Reactions were performed with the 2X SYBR green mix (cat no. KK4601; Kapabiosystems, Inc.) using a fluorescence quantitative PCR instrument (ABI 7500). The PCR primers were synthesized from TsingKe Biological Technology and the sequences were as follows: i) human SERPINA3 forward, 5'-TGGTGCCCA TGATGAGTTTG-3' and reverse, 5'-AACGCACAATGGTCC TTGTC-3'; ii) human β-actin forward, 5'-CCTGGCACCCAG CACAAT-3' and reverse, 5'-GGGCCGGACTCGTCATAC-3'. The β-actin mRNA was used as internal controls. The $2^{-\Delta\Delta Cq}$ method (31) was applied to calculate the relative expression of SERPINA3 gene.

Cell viability and cell proliferation assays. The viability of the lung cancer cell lines after overexpression of SERPINA3 was assessed using the Cell Counting Kit-8 (CCK-8) assay according to the manufacturer's instructions. Briefly, the A549 cells, H157 cells, and H1437 cells that stable transfected overexpressed-SERPINA3 vector or empty-vector were counted by hemocytometry and seeded at $3x10^3$ cells per well in 96-well culture plates and cultured at 37˚C for 24 and 48 h. A total of 10 μl of CCK-8 reagent (cat no. MA0218; Dalian Meilun Biology Technology Co., Ltd.) were added to each well and incubated at 37˚C for another 4 h. The absorbance was measured at 450 nm using a SMR60047 Smart Microplate Reader (USCNK Life Science Co. Ltd.). The experimental samples were repeated three times.

The proliferation of the lung cancer cell lines after overexpression of SERPINA3 was tested by the BeyoClick™ EdU Cell Proliferation Kit with Alexa Fluor 488 (cat no. C0071S; Beyotime Institute of Biotechnology, Inc.). Briefly, the cells were seeded at $6x10^5$ cells per well in six-well culture plates and cultured at 37˚C overnight. Then, the cells were transfected with 3 μg overexpressed-SERPINA3 plasmid or empty-vector with Highgene transfection reagents (cat no. RM09014; ABclonal Technology Co., Ltd.) for 24 h. After transfection, the cells were harvested and the DNA proliferation was determined by incorporating of 5-ethynyl-2'-deoxyuridine (EdU) according to the manufacturer's instructions. The nuclei were stained with 1 ml 1X Hoechst 33342 per well at room temperature for 10 min away from light, and the cells were visualized by a SOPTOP ICX41 fluorescence microscope (Ningbo Sunny Instruments Co., Ltd.).

For sensitivity tests of osimertinib, the cells were seeded at $1x10^4$ cells per well in 96-well culture plates overnight. After transfection of plasmids for 6 h, the cells were treated with 0, 0.5, 1, 5 μM osimertinib (Shanghai TopScience Co., Ltd.) for 24 h, then the cell viability was determined with CCK-8 kits (cat no. CK18; Dojindo Laboratories, Inc.) at 450 nm using a microplate reader (Thermo Scientific Multiskan GO).

Cell growth assay. The growth of the lung cancer cell lines after overexpression of SERPINA3 was detected by colony formation assay. Briefly, the transfected cells were seeded in six-well culture plates at $1x10^3$ cells per well and cultured at 37˚C. The culture medium was changed once weekly and cultured for 14 days at 37˚C. When the number of cells forming a colony was >50, the cells were fixed and stained with 0.1% crystal violet (cat no. C8470; Solarbio Beijing Solarbio Science & Technology Co., Ltd.) for 10 min at room temperature. Images of the colonies were captured and quantified by ImageJ software v1.52 (National Institutes of Health). The experimental samples were repeated three times.

Cell apoptosis assay. The apoptosis rate of the lung cancer cell lines after overexpression of SERPINA3 was evaluated using an Annexin V-FITC/PI apoptosis detection kit (cat no. 401003; BestBio, Inc.) according to the manufacturer's instructions. The transfected cells were cultured for 24 h, and then harvested by low-speed centrifugation and washed with ice-cold PBS. Next, 300 μl of binding buffer was added to the suspended cells, and cells were stained with 5 μl propidium iodide and 5 μl Annexin V-FITC at room temperature for 15 min in the dark. The apoptotic cells were tested by a BD FACSCalibur flow cytometer (BD Biosciences). Finally, the results were interpreted using FlowJo software v10.0 (FlowJo LLC).

Cell migration assay. The migration capacity of the lung cancer cell lines after overexpression of SERPINA3 was detected by wound-healing assays. Briefly, the transfected cells were seeded into six-well plates at $1x10^6$ cells per well and cultured with serum-free medium at 37˚C. After the cell density was near 90%, the monolayer was scratched in a straight line using a new 10-μl pipette tip across the center of the well and washed with sterile PBS. The cells were further cultured with fresh medium for an additional 48 h and were visualized at 0, 24 and 48 h under a microscope. The cellular migration area was analyzed by ImageJ software and the migration rate was calculated using the following formula:

$$\text{Migration rate} = \frac{\text{migration area at 0 h} - \text{migration area at 24 h}}{\text{migration area at 0 h}}$$

or

$$\text{Migration rate} = \frac{\text{migration area at 0 h} - \text{migration area at 48 h}}{\text{migration area at 0 h}}$$

The experimental samples were repeated three times.

Cell invasion assay. The invasion of the lung cancer cell lines after overexpression of SERPINA3 was performed with Transwell assays using 12-μm Transwell chambers. Briefly, the 24-well plates were precoated with Matrigel (cat no. 356234; BD Biosciences) at 37˚C for 2 h. The transfected A549, H157, or H1437 cells at $2.5x10^4$ cells per well in 200 μl of serum-free

media were seeded in the upper chamber, and 500 μl medium containing 10% FBS was into the lower chamber. The chambers were inserted into the plates, and the cells were incubated at 37˚C for 24 h. The cells were fixed with methanol for 20 min at room temperature and stained with 0.1% crystal violet for 15 min at room temperature. Then, the non-invasive cells in the upper chambers were removed with cotton swabs, and images of the invasive cells were captured under an inverted SOPTOP ICX41 fluorescence microscope (Ningbo Sunny Instruments Co., Ltd.) using at least three random fields of view. The experiment was repeated three times. Image-Pro Plus software v6.0 (Media Cybernetics, Inc.) was used to calculate the cellular invasion ability.

In vivo tumorigenic assay. The biological functions of SERPINA3 involved in the occurrence of lung cancer were also evaluated at the animal level. Five-week-old female BALB/c nude mice (n=12; weight, 16-17 g) were purchased from the Experimental Animal Center of China Three Gorges University (permission number: SCXK 2017-0012), and bred under pathogen-free conditions (temperature, 18-22˚C; humidity, 50-60%; 12/12-h light- dark cycle). The animals were fed an autoclaved rodent diet *ad libitum*. The mice bedding, feed and water were replaced every 2 days. All procedures followed the institutional and national guidelines for the care and use of laboratory animals.

The subcutaneous xenograft model of lung cancer was constructed as previously described by Li *et al* (32). Briefly, stably transfected empty-vector pCDH and stably transfected overexpressed-SERPINA3 A549 cells were suspended in 100 μl PBS and inoculated subcutaneously $2x10^6$ cells into the right flanks of nude mice (6 mice in each group), respectively. The body weight of nude mice was monitored every 2 days. After 9 days, the tumors were measured every 2 days with a caliper, and tumor volume (V) was calculated by measuring the length (L) and width (W) and applying the formula $V=(L \times W^2) \times 0.5$. On day 29, two mice were found dead in each group. The cause of death may be due to the marked body weight loss. When the mice began to succumb and were immobile and rigid, and were not in a favorable mental state, the body weight was very low, and certain tumors reached the 1-1.5 cm in diameter, the mice were euthanized according to humane care of animals, anesthetized by intraperitoneal injection of sodium pentobarbital with 150 mg/kg (33). The lung and tumor tissues were excised for further analysis.

Data-independent acquisition mass spectrometry (DIA-MS) for quantitative proteomics detection. The mechanism of SERPINA3 involved in the development of lung cancer was explored, and DIA-MS detection identified the DEPs. Two replicates were performed for mass spectrometry data. Firstly, the H157 cells transfected with empty-vector and overexpressed-SERPINA3 were collected respectively and quickly frozen with liquid nitrogen, then the cell samples were further treated and analyzed by SpecAlly Life Technology Co., LTD (Wuhan, China). The proteins from cell lysis were denatured, reduced, and alkylated with a reaction solution containing 1% sodium deoxycholate, 100 mM Tris-HCl with pH 8.5, 10 mM trichloromethyl phosphate, and 40 mM chloroacetamide by one step at 60˚C for 1 h, and digested with trypsin overnight at 37˚C. The digestion reaction was stopped by trifluoroacetic acid, and the digested peptides were desalted, evaporated, and stored at -20˚C until used.

Secondly, DIA-MS detection and data acquisition was performed using an Orbitrap Exploris 480 Mass Spectrometer coupled with an EASY-NLC 1200 liquid phase LC-MS system, and the parameters were referenced as previously described (34). Peptide samples were aspirated by an autosampler and bound to a C18 analytical column for separation. Mobile phase A consisted of 0.1% formic acid, mobile phase B consisted of 0.1% formic acid, and 80% acetonitrile was used to establish the analytical gradient. The flow rate was maintained at 300 nl/min. The mass spectrometry data was collected with DIA model, and each cycle included one MS1 scan (Max IT was 30 ms, scan range from 350 to 1,250 m/z) and 40 MS2 scans with variable windows (Max IT=50 ms), and the collision energy was set to 30.

Finally, the DIA raw data files of MS detection were analyzed by DIA-NN software v1.8. The human proteome reference database in Uniprot (2021-03-12, containing 20381 protein sequences; uniprot.org) was used for search analysis. The spectrum libraries were obtained via the deep learning algorithm in DIA-NN and MBR function, and the spectrum libraries were used to extract the original DIA data to obtain protein quantitative information. The final results were screened by 1% false discovery rates for parent ion and protein levels. The quality procedures including mass bias, enzyme digestion efficiency, and missing data, have been carried out in the analysis of MS detection data. In the MS data of the present study, the distribution of missing enzyme sites was small, the enzyme digestion efficiency was high, and the proportion of missing data was <0.9%. The quantitative information of the proteome was used for screening and subsequent analysis.

WB. The expression levels of SERPINA3, GAPDH, speckle-type POZ protein (SPOP) and NF-κB p65 in lung cancer cells or tumor tissue samples were detected by WB. Briefly, 15 μg proteins from cell lysates or tissue lysates were measured using a bicinchoninic acid (BCA) protein assay kit (Thermo Fisher Scientific, Inc.) and were subjected to 12% SDS-PAGE. After electrophoresis, the gels were transferred onto PVDF membranes, and the membranes were blocked with 5% BSA (Biofroxx; neoFroxx) in 0.1% TBST (0.1% Tween-20 in 1X TBS) at room temperature (RT) for 1 h. The membranes were probed with polyclonal antibodies against SERPINA3 (1:2,000; cat no. PAB015Hu01; Wuhan USCN Business Co., Ltd.), GAPDH (1:10,000; cat no. 60004-1-Ig; Proteintech Group, Inc.), SPOP (1:10,000; cat no. A19578; ABclonal Technology Co., Ltd.) or NF-κB p65 (1:5,000; cat no. 10745-1-AP; Proteintech Group, Inc.) as primary antibodies, overnight at 4˚C. The membranes were incubated with HRP-conjugated goat-anti-rabbit IgG as the secondary antibody (1:5,000; cat no. 30000-0-AP; Proteintech Group, Inc.) for 1 h at RT and detected by Supersignal West Pico Chemiluminescent HRP Substrate (Bio-Rad Laboratories, Inc.). Images of the data were captured by a Vilber FUSION FX7 chemiluminescence imager. The loading control sample in each gel was used as an internal standard for quantification. Densitometric analysis of each band was measured using ImageJ software, and the data statistics were analyzed by

GraphPad Prism v8.0 software (Dotmatics) with an unpaired t-test.

Bioinformatics analysis. The SERPINA3 expression levels were detected in the HUMAN PROTEIN ATLAS (HPA; https://www.proteinatlas.org/ENSG00000196136-SERPINA3). The mRNA expression levels of SERPINA3 and correlation analysis were detected using the Gene Expression Profiling Interactive Analysis (GEPIA) database (http://gepia.cancer-pku.cn/). The Gene Expression Omnibus (GEO) database was used for analysis of SERPINA3 expression in the osimertinib-resistant NSCLC cell line NCI-H1975 (https://www.ncbi.nlm.nih.gov/geo/query/acc.cgi?acc=GSE201608) (35). The association between the protein expression with tumor stage and immune subtypes in LUAD and LUSC were performed using the TISIDB database (http://cis.hku.hk/TISIDB/). The correlation between protein expression and the survival time of lung cancer patients were tested by Kaplan-Meier Plotter database (http://kmplot.com/analysis/). The TargetScanHuman database (https://www.targetscan.org/vert_72/) was used to identify the target of SERPINA3 mRNA (TargetScanHuman 7.2 predicted targeting of Human SERPINA3).

For MS data, the enrichment analysis of identified 245 proteins was analyzed by ShinyGO v0.76 (http://bioinformatics.sdstate.edu/go/), and the histograms and dot bubble plots of enriched Gene Ontology (GO) terms and pathways were acquired by W-bioinformatics (http://www.bioinformatics.com.cn/). The identified 245 proteins were annotated by GO terms using WEGO (https://biodb.swu.edu.cn/cgi-bin/wego/index.pl). The heat map was analyzed with R v4.2.1 programming tools with the gplots package. The protein-protein interaction networks were constructed using STRING (https://string-db.org/), and the networks were performed by Cytoscape v3.9.1 software (https://cytoscape.org/) (36).

Statistical analysis. The receiver operator characteristic (ROC) curve was constructed by SPSS v26.0 software (IBM Corp.) to analyze the AUC value, sensitivity, and specificity for evaluating the diagnostic performance of SERPINA3. To find the optimum efficiency, Youden index was calculated using the formula: Youden index=sensitivity + specificity-1 (25). The sensitivity and specificity were confirmed when Youden index is maximum.

The correlation between SERPINA3 mRNA expression and LUAD or LUSC was performed by Spearman's correlation analysis. The data of cytological experiments were statistically analyzed by GraphPad Prism v8.0 software with an unpaired t-test, and $P<0.05$ was considered to indicate a statistically significant difference. Data were expressed as the mean ± SD.

Results

The expression level of SERPINA3 is decreased in lung cancer. Through bioinformatic analysis, the expression level of SERPINA3 was measured in several normal tissues. It was found that SERPINA3 mRNA levels were mainly expressed in the liver, pancreas, prostate, urinary bladder, ovary and lung based on the HPA database and GTEx database (Fig. 1A). The protein levels were mainly in the cerebellum, cervix, prostate, liver, pancreas and lung (Fig. 1B). Using the GEPIA database based on The Cancer Genome Atlas dataset and GTEx data, it was determined that SERPINA3 mRNA expression in lung cancer tissues significantly decreased in LUAD (n=347) and LUSC (n=338) compared with normal tissues, as demonstrated in Fig. 1C, which was significantly correlated with tumor stage in LUSC (Fig. 1D; $P<0.001$). Furthermore, in experimental validation, the protein expression level of SERPINA3 was significantly reduced in three lung cancer tissues compared with paracancerous tissues by WB detection ($P=0.0324$) (Fig. 1E and F). In cancer cell lines, it was found that SERPINA3 mRNA was expressed in skin, liver, lung, pancreatic, ovarian, bladder and prostate cancer (Fig. 1G). In lung cancer cell lines, SERPINA3 mRNA was transcribed at lower levels in A549, H157, H1437 and H1975 cells (Fig. 1H). It was also validated that the SERPINA3 protein expression levels were reduced in three lung cancer cell lines (A549, H157 and H1975) (Fig. 1I).

The TargetScanHuman database was also used to analyze the reasons for regulating the SERPINA3 expression, which was found that microRNA-137 (miR-137) is the only miRNA that could bind to the 3'-untranslated region (UTR) of SERPINA3 mRNA as revealed in Fig. S2 (TargetScanHuman 7.2 predicted targeting of Human SERPINA3), which suggests that miR-137 could regulate SERPINA3 mRNA expression.

Overexpression of SERPINA3 suppresses lung cancer at the cellular level. To investigate the role of SERPINA3 in the pathogenesis of lung cancer, three lung cancer cell lines, A549, H157 and H1437 cells that were stably transfected with SERPINA3 overexpression plasmids were constructed by lentiviral transfection. The RT-qPCR results indicated that SERPINA3 was significantly overexpressed in A549, H157 and H1437 cells (Fig. S3). Furthermore, the cytological tests were performed after stable transfection of overexpressed SERPINA3 in lung cancer cells. CCK-8 assays indicated that the cell viability of the three lung cancer cell lines was significantly reduced by ~30% when SERPINA3 was overexpressed compared with the control group at 24 and 48 h (Fig. 2A). Clonogenic assays revealed that the growth of the three lung cancer cell lines was decreased after the overexpression of SERPINA3 (Fig. 2B and C). The fluorescence intensity was weakened when EdU was incorporated into the SERPINA3-overexpressing group, indicating that the DNA proliferation capacity was significantly decreased in these three lung cancer cell lines after overexpression of SERPINA3 ($P<0.01$; Fig. 2D and E).

Moreover, cell apoptosis, migration and invasion were also analyzed in the present study. The proportion of cell apoptosis in the three lung cancer cell lines was significantly higher in SERPINA3-overexpressing cells after flow cytometric analysis (Fig. 3A and B; $P<0.01$). The cell migration rate was assessed with wound-healing assays, and the results showed that the stably transfected SERPINA3-overexpressing cells migrated toward the scratch more slowly in the three lung cancer cell lines at 24 and 48 h (Fig. 3C and D). The cell invasion ability was suppressed after overexpression of SERPINA3 in three stable lung cancer cell lines (Fig. 3E and F; $P<0.05$). Thus, SERPINA3 may have antineoplastic roles in lung cancer *in vitro*.

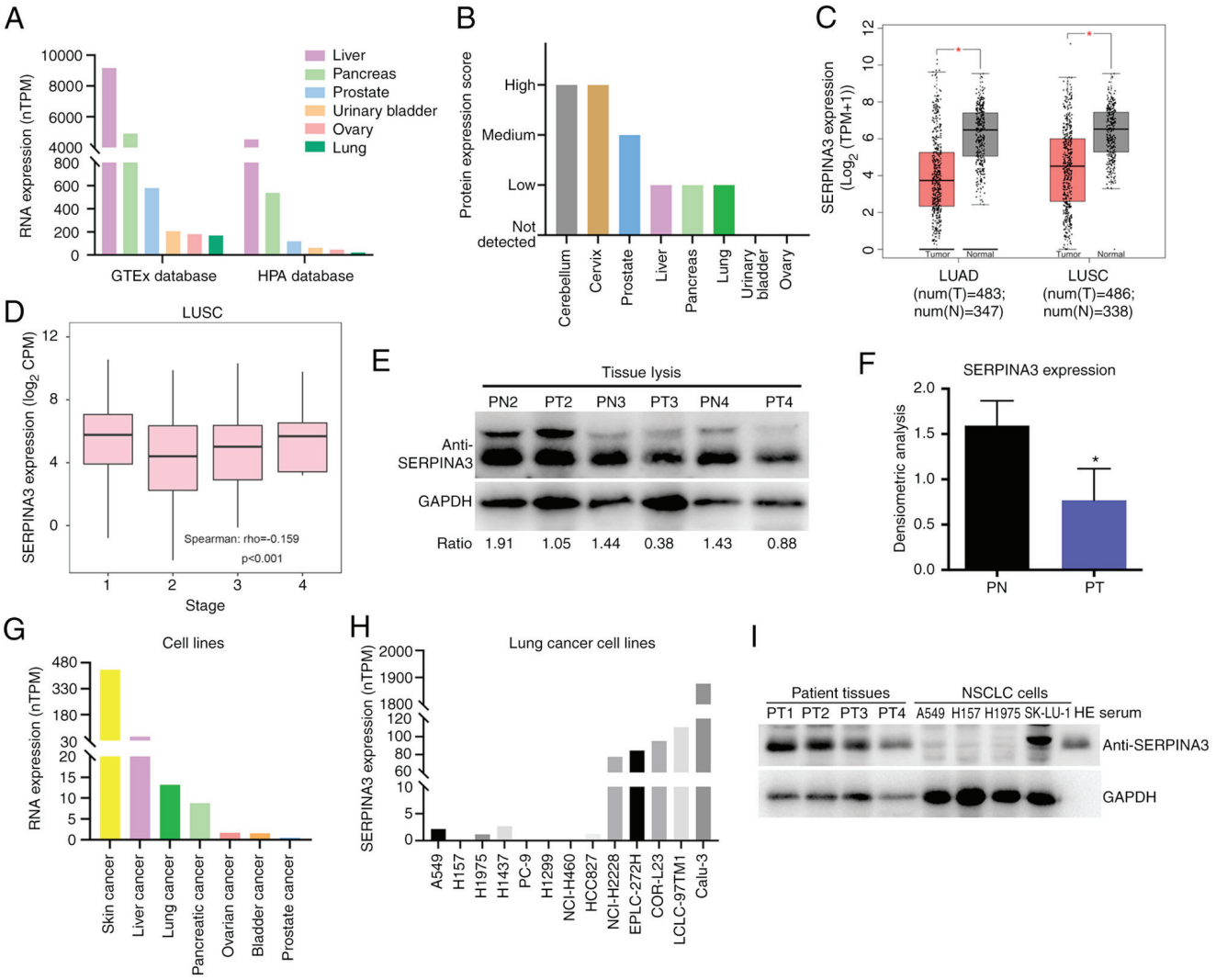

Figure 1. Analysis of SERPINA3 expression levels in lung cancer. (A) Detection of the SERPINA3 mRNA expression level in normal tissues with HPA database. (B) Analysis of the SERPINA3 protein expression level in normal tissues with HPA database. (C) The expression changes of SERPINA3 in lung cancer tissues with the Gene Expression Profiling Interactive Analysis database. Red represents tumor (T) tissues, and gray represents normal (N) tissues. Parameter settings: $|\log_2 FC|$ cutoff: 1; P-value cutoff: 0.01; Log scale: yes, and the $\log_2(TPM + 1)$ was used for log-scale; Jitter size: 0.4; Matched normal data: match The Cancer Genome Atlas normal and GTEx data. (D) The correlation analysis between SERPINA3 protein and tumor stage in LUSC. (E) WB analysis of SERPINA3 expression in lung cancer tissues. (F) The densitometric analysis was measured using ImageJ software. (G) The SERPINA3 mRNA expression level was detected in cancer cell lines with the HPA database. (H) The SERPINA3 mRNA expression level was detected in lung cancer cell lines with HPA database. (I) WB analysis of SERPINA3 expression in lung cancer cell lines. *P<0.05. SERPINA3, serpin family A member 3; HPA, Human Protein Atlas; TPM, transcripts per million; LUAD, lung adenocarcinoma; LUSC, lung squamous cell carcinoma; CPM counts per million; WB, western blotting; PN, paracancerous tissues; PT, patient tumors; WB, western blotting.

Overexpression of SERPINA3 enhances the sensitivity of lung cancer cells to osimertinib. In addition, the Gene Expression Omnibus (GEO) database (GSE201608) was mined and it was found that SERPINA3 expression was decreased ~10-fold in the osimertinib-resistant NSCLC cell line NCI-H1975 in the aformentioned database (GSE201608) (Fig. 4A); therefore, the sensitivity of lung cancer cells to osimertinib after overexpressing SERPINA3 was also detected. The cell viability assays indicated that the H1975 and H157 cells, after transfection of the SERPINA3 overexpression plasmid, were more sensitive to osimertinib, and the H1975 cells were dose-dependent when responding to osimertinib (P<0.05; Fig. 4B and C). However, the H1975 cells showed resistance to osimertinib, maybe the treatment time of osimertinib was not enough in this experiment.

Anticancer effects of overexpressed SERPINA3 in a mouse model of lung cancer. To monitor tumor growth and evaluate the antitumor effect *in vivo*, a xenograft model of lung cancer with BALB/c nude mice (n=6 per group) was also established. A schematic diagram is shown in Fig. 5A. After a few days of feeding, when the BALB/c nude mice weighed 17-18 g, they were subcutaneously injected with stably transfected SERPINA3-overexpressing or empty-vector A549 cells (D1) for subsequent observation and monitoring, and the mice were sacrificed on day 29 after injection. As shown in Fig. 5B, the body weight of tumor-bearing mice decreased significantly and was very light on day 29, and the average weight in the empty-vector group was 10 g (loss of 44.4%); whereas the average weight in the SERPINA3-overexpressing group was 11.8 g (loss of 33.3%). As demonstrated in Fig. 5C, the tumor

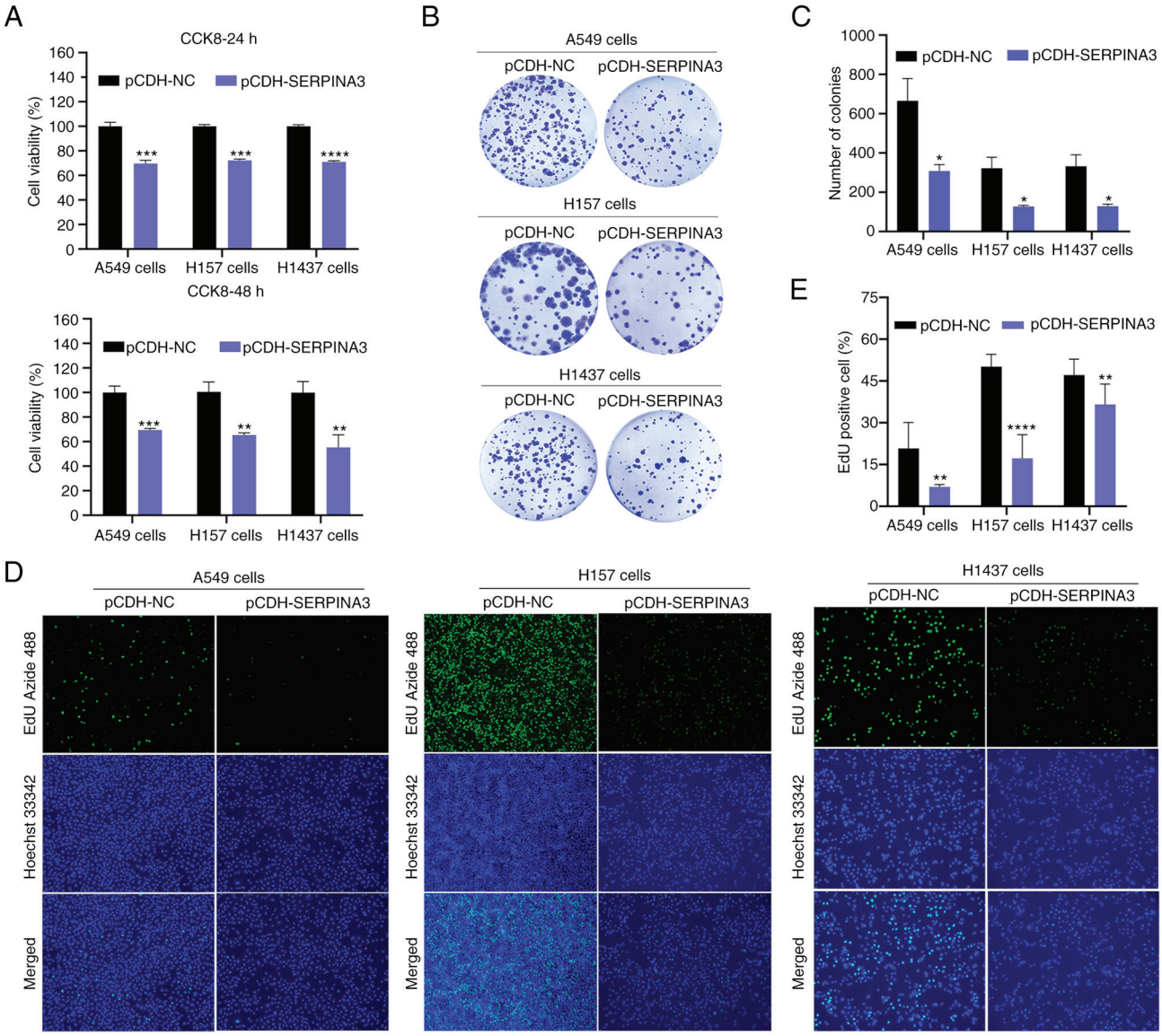

Figure 2. Detection of viability, growth, and proliferation after overexpression of SERPINA3 in three lung cancer cell lines. (A) The cell viability was determined with CCK-8 kits at 24 and 48 h in stably transfected SERPINA3-overexpressing A549, H157 and H1437 cells. (B) Representative colony images of cell growth in the three lung cancer cell lines. (C) Bar charts demonstrating the clonogenic statistical analysis of the three lung cancer cell lines. (D) Cell proliferation was visualized by immunofluorescence detection with EdU assays. (E) Statistical analysis of EdU positive cells. SERPINA3, serpin family A member 3; CCK-8, Cell Counting Kit-8; NC, negative control; EdU, 5-ethynyl-2'-deoxyuridine. *P<0.05, **P<0.01, ***P<0.001 and ****P<0.0001.

volume in the empty-vector group gradually increased and the maximum diameter of tumor reached 11 mm, whereas the tumor-bearing mice in the SERPINA3-overexpressing group developed tumors on the 21st day after injection of tumor cells, which appeared 12 days later than in the empty-vector group. The tumors formed by the SERPINA3-overexpressing cells were smaller in size than those formed by the control cells (Fig. 5D). However, there was no significant difference in tumor weight (P=0.09; Fig. 5F). In the empty-vector group, the morphology of lung tissues was blackened and changed, and the weight of the lung tissues was significantly decreased compared with the SERPINA3-overexpressing group (P=0.0083; Fig. 4E and G).

Overexpressed SERPINA3 upregulates SPOP expression and inhibits NF-κB in lung cancer cells. To further explore the regulatory mechanism of SERPINA3 involved in the development of lung cancer, the DEPs regulated by SERPINA3 were measured with DIA-MS detection. The data for quantitative proteomics detection are available via ProteomeXchange with identifier PXD036119, and detailed information on the proteins identified by MS is shown in Table SII. A total of 7,530 proteins were identified, and the proteins were filtered twice based on the P-value and fold change, as shown in Fig. 6A. Finally, 245 proteins were obtained, and 65 proteins were significantly differentially expressed, of which 46 proteins were upregulated, and 19 proteins were downregulated based on a ratio of pCDH-SERPINA3 to pCDH-NC >1.2 or <0.8 (Table I). The volcano diagram also shows 7479 proteins, of which downregulated proteins are illustrated in blue and upregulated proteins are shown in red (Fig. 6B). GO annotation analysis was performed with 245 identified proteins, as demonstrated in dot-bubble plots (Fig. 6C), and the data are provided in Table SIII. Of these, 18 functions were screened from GO annotation and analyzed by a heatmap.

Figure 3. Detection of apoptosis, migration and invasion after overexpression of SERPINA3 in the three lung cancer cell lines. (A) Flow cytometric analysis of cell apoptosis in the three lung cancer cell lines. (B) Statistical analysis of the percentage of apoptotic cells. (C) Wound-healing assay was performed to observe the role of SERPINA3-overexpressing cells in cell migration. (D) The cell migration rate was analyzed in SERPINA3-overexpressing cells. (E) Invasive cells through the Matrigel-coated membrane in Transwell were stained and visualized by a light microscope. Magnification, x200. (F) The invasive cells were counted in at least three microscopic fields and statistically analyzed. Data were expressed as the mean ± SD. *P<0.05, **P<0.01, ***P<0.001 and ****P<0.0001. SERPINA3, serpin family A member 3.

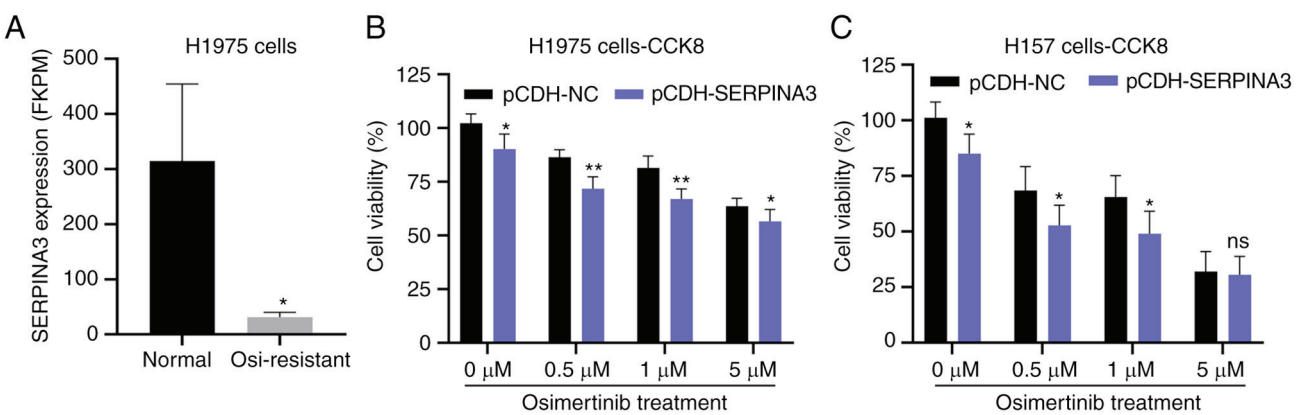

Figure 4. Evaluation of the sensitivity to osimertinib when SERPINA3 was overexpressed in lung cancer cells. (A) Detection of SERPINA3 expression levels in H1975 cells and osimertinib-resistant cells. (B and C) The cell viability was examined with CCK-8 kits after overexpression of SERPINA3 and osimertinib treatment in (B) H1975 and (C) H157 cells. Data were expressed as the mean ± SD. *P<0.05 and **P<0.01. SERPINA3, serpin family A member 3; CCK-8, Cell Counting Kit-8; ns, no significance.

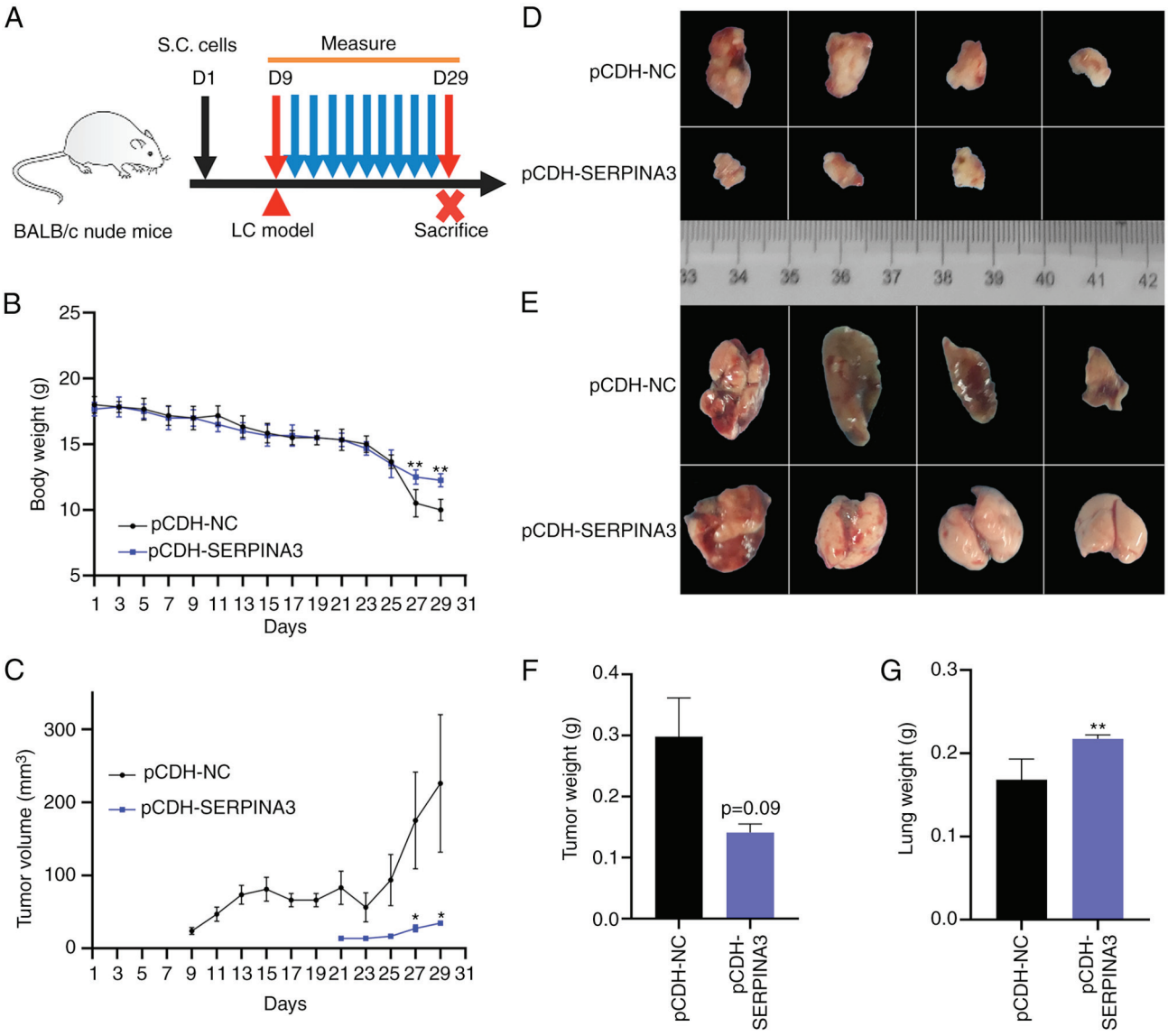

Figure 5. Antitumor effect on tumor-bearing mice after injection of SERPINA3-overexpressing cells. (A) Establishment of subcutaneously xenograft model of lung cancer with BALB/c nude mice. (B) The body weight change of tumor-bearing mice (n=6 in each group). Data were expressed as the mean ± SEM. (C) The tumor volume change of tumor-bearing mice. Data were expressed as the mean ± SEM. (D) The size of tumor tissues. (E) Statistical analysis of weight in tumor tissues. Data were expressed as the mean ± SEM. (F) The morphology of lung tissues. (G) Statistical analysis of weight in lung tissues. Data were expressed as the mean ± SD. *P<0.05 and **P<0.01. SERPINA3, serpin family A member 3.

The identified proteins were related to the nucleolus, catabolic process, response stimulation, signal transduction, cell death, cell cycle, immune, metabolism, and other functions that were significantly changed in lung cancer cells after SERPINA3 overexpression (Fig. 6D and Table SIV). The protein-protein interaction analysis was used by STRING, and the networks were generated using Cytoscape software (Fig. 6E), which identified that SERPINA3 interacted with clusterin and creatine kinase B proteins, and the original data are listed in Table SV. The protein pathway enrichment analysis is also shown in dot-bubble plots with 245 identified proteins (Fig. 6F), which are mainly involved in transcription, multi-organism transport, protein localization and metabolic processes, and the data are provided in Table SIII.

According to the significance fold-change and molecular weight of DEPs, whether their function is involved in lung cancer, and whether they exist in commercial antibodies for detection, SPOP was selected for further analysis. GEPIA database analysis found that SPOP expression had a decreasing trend in LUSC (Fig. S4A). Additionally, the same was reported in LUAD by Dong *et al* (37). TISIDB (http://cis.hku.hk/TISIDB/) database analysis demonstrated that SPOP had no significant correlation with tumor stage in LUAD but had a significant correlation with tumor stage in LUSC (Fig. S4B and C, respectively), and SPOP expression was significantly associated with immune subtype distribution (Fig. S4D and E). Kaplan-Meier Plotter database analysis (http://kmplot.com/analysis/) indicated that the survival time was shorter in lung cancer patients with lower SPOP expression than in those with higher SPOP expression (Fig. 6G). GEPIA database analysis found that SPOP expression was positively correlated with SERPINA3 expression in lung cancer (Fig. 6H). In the MS data of the present study, the protein expression level of SPOP was significantly increased after SERPINA3 overexpression in H157 cells, as shown in Table I.

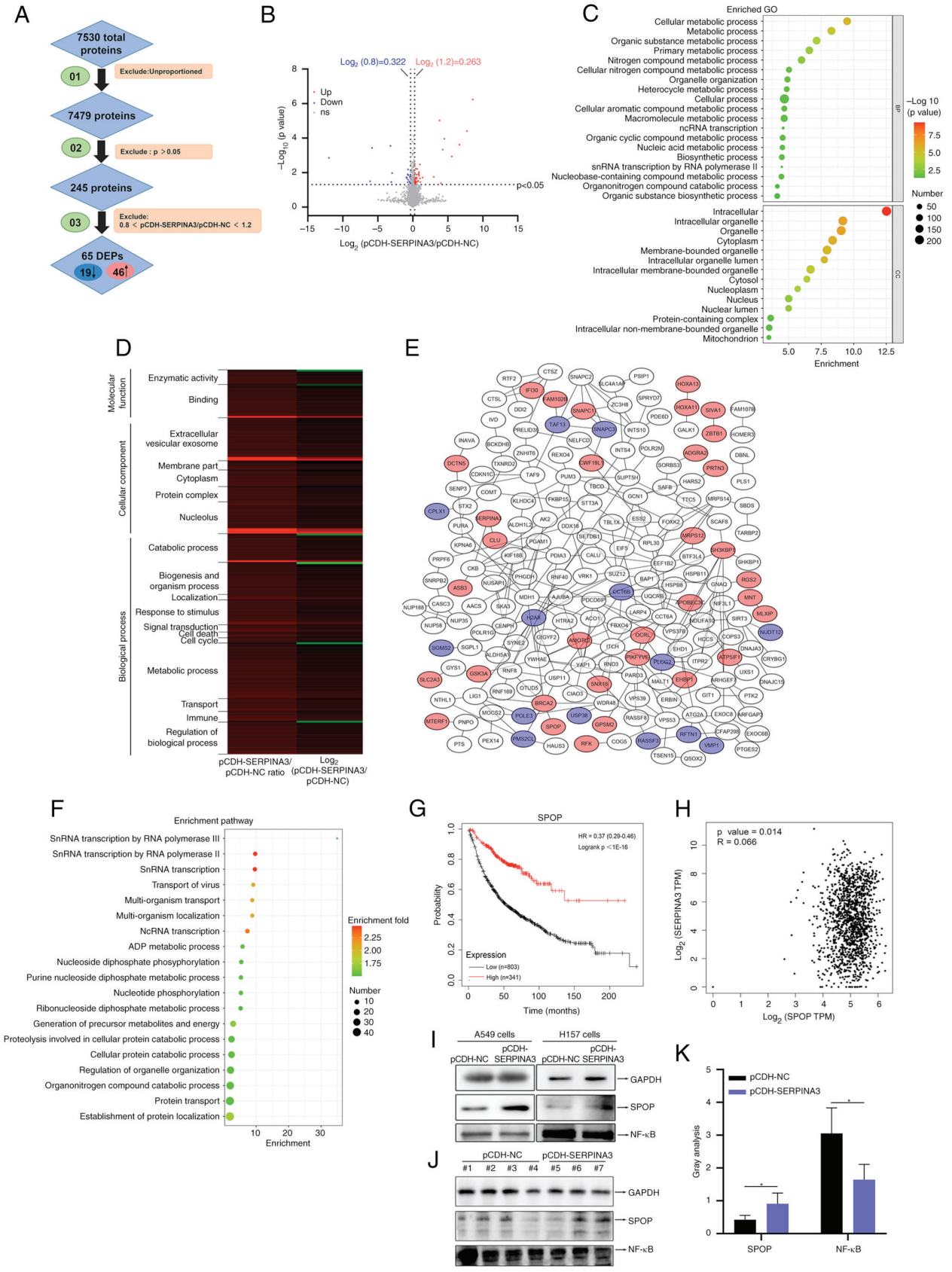

Figure 6. Data-independent acquisition mass spectrometry analysis and WB detection of SPOP and NF-κB expression with SERPINA3 overexpressing lung cancer cells and tumor tissues. (A) Flow chart for protein filtration. (B) Volcano diagram of DEPs analysis. (C) Dot-bubble plots of Gene Ontology annotation analysis. (D) The DEPs involved in 18 functions were analyzed by heat map. (E) Analysis of the protein-protein interaction analysis using Cytoscape software. (F) Dot-bubble plots of the protein pathway enrichment analysis. (G) Survival analysis of SPOP in lung cancer with Kaplan-Meier plotter database. (H) The Gene Expression Profiling Interactive Analysis database was used to analyze the correlation between SPOP and SERPINA3 expression. (I) SPOP and NF-kB p65 expression levels were determined by WB in lung cancer cells. (J) Detection of SPOP and NF-kB p65 expression levels in tumor tissues by WB. (K) Quantification analysis of protein expression levels. Data were expressed as the mean ± SD. *P<0.05. WB, western blotting; SPOP, speckle-type POZ protein; SERPINA3, serpin family A member 3; DEPs, differentially expressed proteins.

Table I. List of the significant differentially expressed proteins by data-independent acquisition mass spectrometry detection.

Accession no. (Uniprot database)	Gene	Description	Molecular weight (kDa)	pCDH-SERPINA3/ pCDH-NC	P-value
Q0VAQ4	SMAGP	Small cell adhesion glycoprotein	10.679	375.241	0.000
P01011	SERPINA3	Alpha-1-antichymotrypsin	47.651	210.880	0.000
P22079	LPO	Lactoperoxidase	80.288	100.793	0.000
P81274	GPSM2	G-protein-signaling modulator 2	76.662	47.806	0.001
O43309	ZSCAN12	Zinc finger and SCAN domain-containing protein 12	70.222	22.863	0.000
P51587	BRCA2	Breast cancer type 2 susceptibility protein	384.202	19.397	0.000
O43791	SPOP	Speckle-type POZ	42.132	16.291	0.042
P11169	SLC2A3	Solute carrier family 2, facilitated glucose transporter member 3	53.924	14.177	0.000
Q96PE1	ADGRA2	Adhesion G protein-coupled receptor A2	142.647	7.983	0.018
P41220	RGS2	Regulator of G-protein signaling 2	24.382	2.630	0.020
Q99551	MTERF1	Transcription termination factor 1, mitochondrial	45.778	2.098	0.036
P31270	HOXA11	Homeobox protein Hox-A11	34.486	2.020	0.003
P24158	PRTN3	Myeloblastin	27.807	2.004	0.022
P13284	IFI30	Gamma-interferon-inducible lysosomal thiol reductase	27.964	1.870	0.015
Q9NRW3	APOBEC3C	DNA dC->dU-editing enzyme APOBEC-3C	22.826	1.844	0.009
Q8NHZ8	CDC26	Anaphase-promoting complex subunit CDC26	9.777	1.791	0.012
Q9Y2I7	PIKFYVE	1-phosphatidylinositol 3-phosphate 5-kinase	237.136	1.729	0.013
Q14CN4	KRT72	Keratin, type II cytoskeletal 72	55.877	1.719	0.030
Q969G6	RFK	Riboflavin kinase	17.623	1.640	0.032
Q86X95	CIR1	Corepressor interacting with RBPJ 1	52.313	1.551	0.006
Q5T8I3	FAM102B	Protein FAM102B	39.308	1.466	0.019
Q9Y2K1	ZBTB1	Zinc finger and BTB domain-containing protein 1	82.016	1.451	0.036
Q8N4S0	CCDC82	Coiled-coil domain-containing protein 82	64.002	1.433	0.013
P31271	HOXA13	Homeobox protein Hox-A13	39.727	1.432	0.023
Q9BTE1	DCTN5	Dynactin subunit 5	20.127	1.357	0.036
Q9UII2	ATP5IF1	ATPase inhibitor, mitochondrial	12.249	1.347	0.033
Q16533	SNAPC1	snRNA-activating protein complex subunit 1	42.994	1.330	0.006
O15304	SIVA1	Apoptosis regulatory protein Siva	18.695	1.321	0.036
Q9HBE1	PATZ1	POZ-, AT hook-, and zinc finger containing protein 1	74.060	1.318	0.038
Q8N954	GPATCH11	G patch domain-containing protein 11	33.277	1.316	0.047
Q99583	MNT	Max-binding protein MNT	62.300	1.290	0.041
Q9Y575	ASB3	Ankyrin repeat and S	57.745	1.285	0.020
P49840	GSK3A	Glycogen synthase kinase-3 alpha	50.981	1.274	0.033
Q96RF0	SNX18	Sorting nexin-18	68.894	1.272	0.046
O15235	MRPS12	28S ribosomal protein S12, mitochondrial	15.173	1.267	0.006

Table I. Continued.

Accession no. (Uniprot database)	Gene	Description	Molecular weight (kDa)	pCDH-SERPINA3/ pCDH-NC	P-value
Q9Y2J4	AMOTL2	Angiomotin-like protein 2	85.764	1.266	0.029
Q9HAP2	MLXIP	MLX-interacting protein	101.185	1.258	0.042
Q01968	OCRL	Inositol polyphosphate 5-phosphatase OCRL	104.205	1.251	0.021
Q12979	ABR	Active breakpoint cluster region-related protein	97.598	1.250	0.037
Q96B97	SH3KBP1	SH3 domain-containing kinase-binding protein 1	73.126	1.240	0.031
Q8NDI1	EHBP1	EH domain-binding protein 1	140.017	1.238	0.011
Q99956	DUSP9	Dual specificity protein phosphatase 9	41.868	1.225	0.040
P10909	CLU	Clusterin	52.495	1.217	0.024
Q69YN2	CWF19L1	CWF19-like protein 1	60.619	1.209	0.039
Q9Y4F5	CEP170B	Centrosomal protein of 170 kDa protein B	171.688	1.206	0.036
Q9H6A9	PCNX3	Pecanex-like protein 3	222.039	1.204	0.003
P17661	DES	Desmin	53.536	0.793	0.041
Q5TCX8	MAP3K21	Mitogen-activated protein kinase kinase kinase 21	113.957	0.790	0.016
P16104	H2AX	Histone H2AX	15.145	0.786	0.043
Q9NRF9	POLE3	DNA polymerase epsilon subunit 3	16.860	0.743	0.018
Q15543	TAF13	Transcription initiation factor TFIID subunit 13	14.287	0.736	0.037
Q2TB18	ASTE1	Protein asteroid homolog 1	77.093	0.721	0.033
P16885	PLCG2	1-phosphatidylinositol 4,5-bisphosphate phosphodiesterase gamma-2	147.870	0.650	0.014
Q0P6H9	TMEM62	Transmembrane protein 62	73.133	0.629	0.026
Q96GC9	VMP1	Vacuole membrane protein 1	46.238	0.620	0.007
Q9BQG2	NUDT12	NAD-capped RNA hydrolase NUDT12	52.076	0.601	0.013
Q14699	RFTN1	Raftlin	63.146	0.598	0.037
O14810	CPLX1	Complexin-1	15.030	0.560	0.021
Q8NB14	USP38	Ubiquitin carboxyl-terminal hydrolase 38	116.546	0.528	0.019
Q86WH2	RASSF3	Ras association domain-containing protein 3	27.562	0.128	0.011
Q68D20	PMS2CL	Protein PMS2CL	20.909	0.119	0.035
Q92966	SNAPC3	snRNA-activating protein complex subunit 3	46.753	0.110	0.000
Q8NHU3	SGMS2	Phosphatidylcholine:ceramide cholinephosphotransferase 2	42.280	0.018	0.000
Q7Z401	DENND4A	C-myc promoter-binding protein	209.244	0.015	0.032
Q92526	CCT6B	T-complex protein 1 subunit zeta-2	57.821	0.000	0.001

Further validation with WB revealed that SPOP expression was upregulated and NF-κb p65 expression was downregulated after overexpression of SERPINA3 in A549 and H157 cells (Fig. 6I). In mouse tumor tissues, SPOP expression was significantly increased (P=0.0390), and NF-κB p65 expression (P=0.0396) was significantly decreased (Fig. 6J and K).

Discussion

Elucidating the complex pathogenesis of lung cancer is of great significance for drug development and improvement of the survival rate, which is a promising study area. Aiming at gene alterations, including epidermal growth factor receptor mutation, Kirsten rat sarcoma viral homolog mutation (7,38), epigenetic regulation (39,40) and tumor microenvironment regulation (41), as well as uncontrolled signaling pathways such as the MEK/ERK signaling pathway (42) and PI3K/AKT signaling pathway (43), numerous drugs have been developed and used for the treatment of lung cancer (44,45). In addition, current research has found that certain novel genes are involved in the occurrence and development of lung cancer; for example, MG53 suppressed tumor progression by modulating G3BP2 activity in NSCLC (32), which is a potential therapeutic target for lung cancer. Therefore, elucidating the pathogenesis of lung cancer will be helpful for lung cancer treatment.

In the present study, the biological effects of SERPINA3 in the occurrence of lung cancer were clarified. *In vitro*, a series of cytological experiments indicated that the proliferation, growth, migration and invasion of lung cancer cells were inhibited, and cell apoptosis was promoted after overexpression of SERPINA3. *In vivo*, animal experiments showed that tumor growth was slower in tumor-bearing mice after the injection of SERPINA3 overexpressing A549 cells. In addition, it was found that lung cancer cells were more sensitive to osimertinib after SERPINA3 overexpression. The present study demonstrated that overexpressed SERPINA3 could act against lung cancer, indicating that SERPINA3 may have an antineoplastic role in lung cancer, and SERPINA3 is also a noteworthy target for the treatment of lung cancer. To date, no available agents targeting SERPINA3 have been reported for tumor treatment.

SERPINA3 is expressed differently in different tumor tissues, and the possible reasons have been reported in a previous publication by the authors; abnormal expression in lung cancer may be due to genetic alterations or immunological regulation (16). The gene changes of SERPINA3 were different in tissue subtypes of lung cancer; for example, the point mutation was 3.48% in LUAD and 2.61% in LUSC by the COSMIC database in the authors' previous analysis (16), which may lead to abnormal expression of SERPINA3 in LUAD and LUSC. In addition, immune cells are closely related to lung cancer occurrence (46). The infiltrated immune cells, such as $CD8^+$ T cells, NK cells, neutrophils and macrophages in the tumor, were significantly correlated with SERPINA3 expression in lung cancer (16). Zhang *et al* (47) have reported that higher SERPINA3 expression was detected in urine of patients with lung cancer at Stage IV. By contrast, it was found that SERPINA3 expression decreased in sera of patients with lung cancer at the early stage, subsequently recovered, and even slightly increased in the late stage, which is probably due to the complexity of regulation in the development of tumors, as previously reported (25). In the present study, the mRNA and protein expression levels of SERPINA3 in lung cancer tissues were decreased based on bioinformatics analysis and experimental validation. In the current experiment, the early-stage tissue samples were used for detection of the expression level of SERPINA3 by WB, and the lung cancer tissues at the late stage were not collected and detected. The different expression level of SERPINA3 in tissues may be associated with collected samples at various stages, tissue subtypes, glycosylation modifications, or immunomodulation. However, the detailed mechanism of abnormal SERPINA3 expression in lung cancer remains unclear and needs further elucidation by experiments.

In addition, TargetScanHuman database analysis indicated that miR-137 could regulate SERPINA3 mRNA expression. The current study also found that miR-137 was a tumor suppressor in human NSCLC (48,49). Chang *et al* (50) reported that upregulation of miR-137 expression could promote cell migration in lung cancer. Whether miR-137 alters the cellular SERPINA3 expression levels in lung cancer, resulting in SERPINA3 involvement in lung cancer occurrence, has not been reported and needs further exploration.

SPOP is a member of the E3 ubiquitin ligase complex with a molecular weight of 42.132 kDa, which is an adaptor that connects the cullin 3 RING ligase to its substrates for mediating the ubiquitin-proteasome degradation pathway (51,52). It was identified that SPOP played an essential role in tumorigenesis and cancer progression (53,54); for example, silencing SPOP accelerated the malignancy of breast cancer (55), and SPOP suppressed tumorigenesis during lung cancer progression (56,57). SPOP inactivation, activation, amplification, and mislocalization contribute to cancer pathogenesis, which is frequently mutated in solid tumors; the mutation patterns and biological consequences are different in cancers (58). The regulation of SPOP expression at different levels includes DNA methylation that affects transcription, miRNAs that affect translation, and phosphorylation and self-ubiquitination that affect post-transcriptional modifications (57). For example, the transcription factor C/EBPα can bind the SPOP promoter; the combination of this transcriptional regulatory element and DNA methylation regulates the expression and function of SPOP in NSCLC (59). MiR-520b is upregulated in NSCLC, and directly targets SPOP 3'-UTR and decreases SPOP expression to promote proliferation and metastasis (60). In lung cancer, there are few studies about the post-transcriptional modifications to regulate the SPOP expression.

In the present study, the expression level of SPOP increased 16-fold in lung cancer cells after SERPINA3 overexpression by DIA-MS detection, and it was further validated that the expression of SPOP was upregulated with WB in lung cancer cells and tumor tissues of mice. In addition, SPOP could promote FAS-associated protein with death domain degradation and inhibit NF-κB activity in NSCLC (61). Previous studies have also indicated that inhibiting the NF-κB signaling pathway is a promising strategy for treating lung cancer (62,63). The present study demonstrated that NF-κB p65 expression was downregulated in lung cancer. The aforementioned results indicated that the overexpression of SERPINA3 suppresses tumor progression by modulating SPOP/NF-κB in lung cancer, suggesting that SERPINA3 is involved in the pathogenesis of lung cancer.

However, there are limitations to the present study. First, the reasons for SERPINA3 expression changes in lung cancer are unknown. Second, the viability of lung cancer cells after knockdown of SERPINA3 expression to explain the biological effects of SERPINA3 in lung cancer was not assessed. In

addition, whether miR-137 alters SERPINA3 expression levels in lung cancer or whether SERPINA3 directly interacts with SPOP to regulate its expression remains unclear. These questions deserve further investigation.

In summary, the present results showed that SERPINA3 was reduced in lung cancer, and overexpressed SERPINA3 exerted antitumoral properties at the cellular and animal levels, which suppressed the tumor growth of lung cancer by activating SPOP expression and inhibiting NF-κB in cell culture systems and *in vivo* models. The present study revealed the antineoplastic role of SERPINA3 in lung cancer and demonstrated that SERPINA3 is involved in lung cancer occurrence, which will promote in-depth elucidation of the pathogenesis of lung cancer and provide a new direction for lung cancer treatment.

Acknowledgements

The authors would like to thank Professor Hui Sun (Wuhan University, Wuhan, China) for her helpful suggestions and providing the SERPINA3 plasmid on the study.

Funding

The present study was supported by the National Natural Science Foundation of China (NSFC) program (grant no. 32000908), the Natural Science Foundation of Hubei Province program (grant no. 2020CFB417), the Hubei Key Laboratory of Edible Wild Plants Conservation and Utilization (grant nos. EWPL202002, EWPL202106 and EWPL202211), and the National innovation and entrepreneurship training program for college students (grant no. 202210513012).

Availability of data and materials

The datasets used and/or analyzed during the current study are available from the corresponding author upon reasonable request. The mass spectrometry proteomics data have been deposited to the ProteomeXchange Consortium via the PRIDE partner repository with the dataset identifier PXD036119.

Authors' contributions

YJ and WW conceptualized the study. YJ, YZ and YC developed methodology. YJ and WD performed formal analysis. YJ, AH, JW, NL, XW and WD conducted investigation. AH and YG provided resources. YJ and YG curated data. YJ and WD wrote the original draft. WD and JP wrote, reviewed and edited the manuscript. YJ, YZ and AH performed visualization. WD and JP supervised the study. YJ and WD acquired funding. YJ, YZ, AH, YG and WD confirm the authenticity of all the raw data. All authors have read and approved the final version of the manuscript.

Ethics approval and consent to participate

The study was conducted according to the Declaration of Helsinki. Human sample collection and animal experiments were approved (approval no. KL901372) by the Research Ethics Board of Nanjing Medical University and the Ethics Committee of Suzhou Municipal Hospital. All the animal experiments were carried out under the Guide for Care and Use of Laboratory Animals, and all methods are reported in accordance with ARRIVE guidelines for animal experiments.

Patient consent for publication

Not applicable.

Competing interests

The authors declare that they have no competing interests.

References

1. Sung H, Ferlay J, Siegel RL, Laversanne M, Soerjomataram I, Jemal A and Bray F: Global cancer statistics 2020: GLOBOCAN estimates of incidence and mortality worldwide for 36 cancers in 185 countries. CA Cancer J Clin 71: 209-249, 2021.
2. Howlader N, Forjaz G, Mooradian MJ, Meza R, Kong CY, Cronin KA, Mariotto AB, Lowy DR and Feuer EJ: The effect of advances in lung-cancer treatment on population mortality. N Engl J Med 383: 640-649, 2020.
3. Kleczko EK, Kwak JW, Schenk EL and Nemenoff RA: Targeting the complement pathway as a therapeutic strategy in lung cancer. Front Immunol 10: 954, 2019.
4. Su L, Chen M, Su H, Dai Y, Chen S and Li J: Postoperative chemoradiotherapy is superior to postoperative chemotherapy alone in squamous cell lung cancer patients with limited N2 lymph node metastasis. BMC Cancer 19: 1023, 2019.
5. Herbst RS, Morgensztern D and Boshoff C: The biology and management of non-small cell lung cancer. Nature 553: 446-454, 2018.
6. Kinoshita T and Goto T: Molecular Mechanisms of pulmonary fibrogenesis and its progression to lung cancer: A review. Int J Mol Sci 20: 1461, 2019.
7. Mascaux C, Tsao MS and Hirsch FR: Genomic testing in lung cancer: Past, present, and future. J Natl Compr Canc Netw 16: 323-334, 2018.
8. Wang M, Herbst RS and Boshoff C: Toward personalized treatment approaches for non-small-cell lung cancer. Nat Med 27: 1345-1356, 2021.
9. Reck M, Carbone DP, Garassino M and Barlesi F: Targeting KRAS in non-small-cell lung cancer: Recent progress and new approaches. Ann Oncol 32: 1101-1110, 2021.
10. Lim JU, Lee E, Lee SY, Cho HJ, Ahn DH, Hwang Y, Choi JY, Yeo CD, Park CK and Kim SJ: Current literature review on the tumor immune micro-environment, its heterogeneity and future perspectives in treatment of advanced non-small cell lung cancer. Transl Lung Cancer Res 12: 857-876, 2023.
11. Martinez-Ruiz C, Black JRM, Puttick C, Hill MS, Demeulemeester J, Larose Cadieux E, Thol K, Jones TP, Veeriah S, Naceur-Lombardelli C, *et al*: Genomic-transcriptomic evolution in lung cancer and metastasis. Nature 616: 543-552, 2023.
12. Garon EB, Hellmann MD, Rizvi NA, Carcereny E, Leighl NB, Ahn MJ, Eder JP, Balmanoukian AS, Aggarwal C, Horn L, *et al*: Five-Year overall survival for patients with advanced non-small-cell lung cancer treated with pembrolizumab: Results from the phase I KEYNOTE-001 study. J Clin Oncol 37: 2518-2527, 2019.
13. Li T, Pan K, Ellinwood AK and Cress RD: Survival trends of metastatic lung cancer in california by age at diagnosis, gender, Race/Ethnicity, and histology, 1990-2014. Clin Lung Cancer 22: e602-e611, 2021.
14. Fatima S, Gupta S, Khan AB, Rehman SU and Jairajpuri MA: Identification and validation of two alternatively spliced novel isoforms of human alpha-1-antichymotrypsin. Biochem Biophys Res Commun 628: 25-31, 2022.
15. Mateusz de Mezer, Rogalinski J, Przewozny S, Chojnicki M, Niepolski L, Sobieska M and Przystanska A: SERPINA3: Stimulator or Inhibitor of Pathological Changes. Biomedicines 11: 156, 2023.

16. Jin Y, Wang W, Wang Q, Zhang Y, Zahid KR, Raza U and Gong Y: Alpha-1-antichymotrypsin as a novel biomarker for diagnosis, prognosis, and therapy prediction in human diseases. Cancer Cell Int 22: 156, 2022.
17. Kim H, Leng K, Park J, Sorets AG, Kim S, Shostak A, Embalabala RJ, Mlouk K, Katdare KA, Rose IVL, *et al*: Reactive astrocytes transduce inflammation in a blood-brain barrier model through a TNF-STAT3 signaling axis and secretion of alpha 1-antichymotrypsin. Nat Commun 13: 6581, 2022.
18. Schneider MA, Rozy A, Wrenger S, Christopoulos P, Muley T, Thomas M, Meister M, Welte T, Chorostowska-Wynimko J and Janciauskiene S: Acute phase proteins as early predictors for immunotherapy response in advanced NSCLC: An explorative study. Front Oncol 12: 772076, 2022.
19. Brioschi M, Gianazza E, Agostoni P, Zoanni B, Mallia A and Banfi C: Multiplexed mrm-based proteomics identified multiple biomarkers of disease severity in human heart failure. Int J Mol Sci 22, 2021.
20. Horta-López PH, Mendoza-Franco G, Rodríguez-Cruz F, Torres-Cruz FM, Hernández-Echeagaray E, Jarero-Basulto JJ, Rícny J, Florán Garduño B and Garcia-Sierra F: Association of α-1-Antichymotrypsin expression with the development of conformational changes of tau protein in Alzheimer's disease brain. Neuroscience 518: 83-100, 2023.
21. Kim KH, Park GW, Jeong JE, Ji ES, An HJ, Kim JY and Yoo JS: Parallel reaction monitoring with multiplex immunoprecipitation of N-glycoproteins in human serum for detection of hepatocellular carcinoma. Anal Bioanal Chem 411: 3009-3019, 2019.
22. Lara-Velazquez M, Zarco N, Carrano A, Phillipps J, Norton ES, Schiapparelli P, Al-Kharboosh R, Rincon-Torroella J, Jeanneret S, Corona T, *et al*: Alpha 1-antichymotrypsin contributes to stem cell characteristics and enhances tumorigenicity of glioblastoma. Neuro Oncol 23: 599-610, 2021.
23. Zhu H, Liu Q, Tang J, Xie Y, Xu X, Huang R, Zhang Y, Jin K and Sun B: Alpha1-ACT functions as a tumour suppressor in hepatocellular carcinoma by inhibiting the PI3K/AKT/mTOR signalling pathway via activation of PTEN. Cell Physiol Biochem 41: 2289-2306, 2017.
24. Zhang Y, Tian J, Qu C, Peng Y, Lei J, Li K, Zong B, Sun L and Liu S: Overexpression of SERPINA3 promotes tumor invasion and migration, epithelial-mesenchymal-transition in triple-negative breast cancer cells. Breast Cancer 28: 859-873, 2021.
25. Jin Y, Wang J, Ye X, Su Y, Yu G, Yang Q, Liu W, Yu W, Cai J, Chen X, *et al*: Identification of GlcNAcylated alpha-1-antichymotrypsin as an early biomarker in human non-small-cell lung cancer by quantitative proteomic analysis with two lectins. Br J Cancer 114: 532-44, 2016.
26. Jin Y, Yang Y, Su Y, Ye X, Liu W, Yang Q, Wang J, Fu X, Gong Y and Sun H: Identification a novel clinical biomarker in early diagnosis of human non-small cell lung cancer. Glycoconj J 36: 57-68, 2019.
27. Seijo LM, Peled N, Ajona D, Boeri M, Field JK, Sozzi G, Pio R, Zulueta JJ, Spira A, Massion PP, *et al*: Biomarkers in lung cancer screening: Achievements, promises, and challenges. J Thorac Oncol 14: 343-357, 2019.
28. Wadowska K, Bil-Lula I, Trembecki L and Sliwinska-Mosson M: Genetic markers in lung cancer diagnosis: A Review. Int J Mol Sci 21: 4569, 2020.
29. Kang K, Niu B, Wu C, Hua J and Wu J: The construction and application of lentiviral overexpression vector of goat miR-204 in testis. Res Vet Sci 130: 52-58, 2020.
30. Liu H, Cheng Q, Xu DS, Wang W, Fang Z, Xue DD, Zheng Y, Chang AH and Lei YJ: Overexpression of CXCR7 accelerates tumor growth and metastasis of lung cancer cells. Respir Res 21: 287, 2020.
31. Livak KJ and Schmittgen TD: Analysis of relative gene expression data using real-time quantitative PCR and the 2(-Delta Delta C(T)) method. Methods 25: 402-408, 2001.
32. Li H, Lin PH, Gupta P, Li X, Zhao SL, Zhou X, Li Z, Wei S, Xu L, Han R, *et al*: MG53 suppresses tumor progression and stress granule formation by modulating G3BP2 activity in non-small cell lung cancer. Mol Cancer 20: 118, 2021.
33. Laferriere CA and Pang DS: Review of intraperitoneal injection of sodium pentobarbital as a method of euthanasia in laboratory rodents. J Am Assoc Lab Anim Sci 59: 254-263, 2020.
34. Zhang F, Ge W, Ruan G, Cai X and Guo T: Data-Independent acquisition mass spectrometry-based proteomics and software tools: A glimpse in 2020. Proteomics 20: e1900276, 2020.
35. Murakami Y, Kusakabe D, Watari K, Kawahara A, Azuma K, Akiba J, Taniguchi M, Kuwano M and Ono M: AXL/CDCP1/SRC axis confers acquired resistance to osimertinib in lung cancer. Sci Rep 12: 8983, 2022.
36. Shannon P, Markiel A, Ozier O, Baliga NS, Wang JT, Ramage D, Amin N, Schwikowski B and Ideker T: Cytoscape: A software environment for integrated models of biomolecular interaction networks. Genome Res 13: 2498-2504, 2003.
37. Dong Y, Zhang D, Cai M, Luo Z, Zhu Y, Gong L, Lei Y, Tan X, Zhu Q and Han S: SPOP regulates the DNA damage response and lung adenocarcinoma cell response to radiation. Am J Cancer Res 9: 1469-1483, 2019.
38. Rubio K, Romero-Olmedo AJ, Sarvari P, Swaminathan G, Ranvir VP, Rogel-Ayala DG, Cordero J, Gunther S, Mehta A, Bassaly B, *et al*: Non-canonical integrin signaling activates EGFR and RAS-MAPK-ERK signaling in small cell lung cancer. Theranostics 13: 2384-2407, 2023.
39. Fan T, Zhu M, Muhammad S, Xiao C, Li S, Tian H, Liu Y, Xue L, Zheng B, Li C, *et al*: H3K4me3-related lncRNAs signature and comprehensive analysis of H3K4me3 regulating tumor immunity in lung adenocarcinoma. Respir Res 24: 122, 2023.
40. Wu J, Feng J, Zhang Q, He Y, Xu C, Wang C and Li W: Epigenetic regulation of stem cells in lung cancer oncogenesis and therapy resistance. Front Genet 14: 1120815, 2023.
41. Srivastava S, Mohanty A, Nam A, Singhal S and Salgia R: Chemokines and NSCLC: Emerging role in prognosis, heterogeneity, and therapeutics. Semin Cancer Biol 86: 233-246, 2022.
42. Yuan J, Ju Q, Zhu J, Jiang Y, Yang X, Liu X, Ma J, Sun C and Shi J: RASSF9 promotes NSCLC cell proliferation by activating the MEK/ERK axis. Cell Death Discov 7: 199, 2021.
43. Jin Y, Chen Y, Tang H, Hu X, Hubert SM, Li Q, Su D, Xu H, Fan Y, Yu X, *et al*: Activation of PI3K/AKT pathway is a potential mechanism of treatment resistance in small cell lung cancer. Clin Cancer Res 28: 526-539, 2022.
44. Lu S, Zhou J, Jian H, Wu L, Cheng Y, Fan Y, Fang J, Chen G, Zhang Z, Lv D, *et al*: Befotertinib (D-0316) versus icotinib as first-line therapy for patients with EGFR-mutated locally advanced or metastatic non-small-cell lung cancer: A multicentre, open-label, randomised phase 3 study. Lancet Respir Med S2213-2600, 00183-2, 2023.
45. Ghiringhelli F, Bibeau F, Greillier L, Fumet JD, Ilie A, Monville F, Lauge C, Catteau A, Boquet I, Majdi A, *et al*: Immunoscore immune checkpoint using spatial quantitative analysis of CD8 and PD-L1 markers is predictive of the efficacy of anti-PD1/PD-L1 immunotherapy in non-small cell lung cancer. EBioMedicine 92: 104633, 2023.
46. Stankovic B, Bjorhovde HAK, Skarshaug R, Aamodt H, Frafjord A, Muller E, Hammarstrom C, Beraki K, Baekkevold ES, Woldbaek PR, *et al*: Immune cell composition in human non-small cell lung cancer. Front Immunol 9: 3101, 2018.
47. Zhang Y, Li Y, Qiu F and Qiu Z: Comparative analysis of the human urinary proteome by 1D SDS-PAGE and chip-HPLC-MS/MS identification of the AACT putative urinary biomarker. J Chromatogr B Analyt Technol Biomed Life Sci 878: 3395-401, 2010.
48. Nuzzo S, Catuogno S, Capuozzo M, Fiorelli A, Swiderski P, Boccella S, de Nigris F and Esposito CL: Axl-Targeted Delivery of the Oncosuppressor miR-137 in Non-small-Cell Lung Cancer. Mol Ther Nucleic Acids 17: 256-263, 2019.
49. Zhang B, Liu T, Wu T, Wang Z, Rao Z and Gao J: microRNA-137 functions as a tumor suppressor in human non-small cell lung cancer by targeting SLC22A18. Int J Biol Macromol 74: 111-8, 2015.
50. Chang TH, Tsai MF, Gow CH, Wu SG, Liu YN, Chang YL, Yu SL, Tsai HC, Lin SW, Chen YW, *et al*: Upregulation of microRNA-137 expression by Slug promotes tumor invasion and metastasis of non-small cell lung cancer cells through suppression of TFAP2C. Cancer Lett 402: 190-202, 2017.
51. Li XM, Wu HL, Xia QD, Zhou P, Wang SG, Yu X and Hu J: Novel insights into the SPOP E3 ubiquitin ligase: From the regulation of molecular mechanisms to tumorigenesis. Biomed Pharmacother 149: 112882, 2022.
52. Shi L, Yan Y, He Y, Yan B, Pan Y, Orme JJ, Zhang J, Xu W, Pang J and Huang H: Mutated SPOP E3 ligase promotes 17betaHSD4 protein degradation to drive androgenesis and prostate cancer progression. Cancer Res 81: 3593-3606, 2021.
53. Zhang H, Jin X and Huang H: Deregulation of SPOP in cancer. Cancer Res 83: 489-499, 2023.
54. Zhou P, Chang WY, Gong DA, Huang LY, Liu R, Liu Y, Xia J, Wang K, Tang N and Huang AL: O-GlcNAcylation of SPOP promotes carcinogenesis in hepatocellular carcinoma. Oncogene 42: 725-736, 2023.

55. Wei C, Liu Y, Liu X, Cheng J, Fu J, Xiao X, Moses RE, Li X and Fu J: The speckle-type POZ protein (SPOP) inhibits breast cancer malignancy by destabilizing TWIST1. Cell Death Discov 8: 389, 2022.
56. Song Y, Xu Y, Pan C, Yan L, Wang ZW and Zhu X: The emerging role of SPOP protein in tumorigenesis and cancer therapy. Mol Cancer 19: 2, 2020.
57. Yang X and Zhu Q: SPOP in Cancer: Phenomena, mechanisms and its role in therapeutic implications. Genes (Basel) 13: 2051, 2022.
58. Cuneo MJ and Mittag T: The ubiquitin ligase adaptor SPOP in cancer. FEBS J 286: 3946-3958, 2019.
59. Yao S, Chen X, Chen J, Guan Y, Liu Y, Chen J and Lv X: Speckle-type POZ protein functions as a tumor suppressor in non-small cell lung cancer due to DNA methylation. Cancer Cell Int 18: 213, 2018.
60. Liu X, Liu J, Zhang X, Tong Y and Gan X: MiR-520b promotes the progression of non-small cell lung cancer through activating Hedgehog pathway. J Cell Mol Med 23: 205-215, 2019.
61. Luo J, Chen B, Gao CX, Xie HK, Han CN and Zhou CC: SPOP promotes FADD degradation and inhibits NF-κB activity in non-small cell lung cancer. Biochem Biophys Res Commun 504: 289-294, 2018.
62. Wang Y, Zhang J, Li YJ, Yu NN, Liu WT, Liang JZ, Xu WW, Sun ZH, Li B and He QY: MEST promotes lung cancer invasion and metastasis by interacting with VCP to activate NF-κB signaling. J Exp Clin Cancer Res 40: 301, 2021.
63. Rasmi RR, Sakthivel KM and Guruvayoorappan C: NF-κB inhibitors in treatment and prevention of lung cancer. Biomed Pharmacother 130: 110569, 2020.